

[3] Approximation of the encircled energy function for the far-field diffraction of a plane light wave by planar complex-shaped apertures



I.M. Sizova

P.N. Lebedev Physics Institute Russian Academy of Sciences, Moscow, Russia

Abstract

A method for approximating the encircled energy in a definite solid angle in the Fraunhofer region by the simulation of the optical transfer function derivative is proposed. The selection of free model parameters allow one to obtain a valid expansion of the encircled energy at the origin of the angular coordinate and at infinity, providing a good approximation in the intermediate domain.

Keywords: APERTURES, DIFFRACTION, DIFFRACTION THEORY.

Citation: SIZOVA I.M. APPROXIMATION OF THE ENCIRCLED ENERGY FUNCTION FOR THE FAR-FIELD DIFFRACTION OF A PLANE LIGHT WAVE BY PLANAR COMPLEX-SHAPED APERTURES / COMPUTER OPTICS. – 2015. – Vol. 39(5). – P. 635-643.

Introduction

The encircled energy in a definite solid angle in the Fraunhofer zone under the diffraction of plane light wave on plane apertures of arbitrary shapes with arbitrary incident fields is calculated as the integral transformation of angle-averaged aperture optical transfer function with a core in the form of the first-order Bessel function. Such problems can arise in different areas of physics, i.e. astronomy, photodissociation lasers with open-discharge emission pumping [1], etc. Calculations of these integrals with the oscillating function are not simple. The solution of inverse problems is even more difficult. Since it is often quite enough to have 10-15% of encircled energy calculation accuracy, it becomes relevant to search its close approximation. We proposed such approximation in papers [2-3], however its accuracy may be acceptable only if there are some restrictions on the shape of apertures and the structure of the incident field. The field should be smooth, and the apertures are not to be very rugged. This paper offers the approximation of encircled energy based on another model if compared with that one shown in [2-3]. It allows us to obtain a higher accuracy of the approximation within a larger range of fields and apertures, and it has apparently good prospects of further improvement within the framework of the offered approach.

1. Basic relationships

In the classical diffraction problem of arbitrary monochromatic light wave incident along the z – axis perpendicular to finite plane aperture ($z = 0$), let us consider the encircled energy $\varepsilon(\vartheta)$ within the cone with a generator at the angle ϑ to z normalized by

$$E_{\Sigma} = \iint |U(\vec{r}, 0)|^2 d^2\vec{r}$$

– the whole flow through apertures, $U(\vec{r}, 0)$ – the field on the aperture with Cartesian coordinates $\vec{r} = \{x, y\}$, Σ – the aperture area.

The expression for the encircled energy $\varepsilon(\vartheta)$ behind apertures in a paraxial region of the Fraunhofer zone obtained in the framework of physical optics by means of the Kirchhoff method in the Fresnel approximation [4-5] is written as follows [2, 6]

$$\varepsilon(\vartheta) = \frac{2\pi\vartheta}{\lambda} \int \bar{T}(\rho) J_1\left(\frac{2\pi\vartheta}{\lambda}\rho\right) d\rho \quad (1)$$

Here λ – is the wavelength; J_1 – is the 1st order Bessel function; $\bar{T}(\rho)$ – is the optical transfer function (OTF) averaged by the ϕ -angle of the polar coordinates $\vec{\rho} = \{\rho, \phi\}$ entered into aperture planes in place of the Cartesian coordinates

$$\bar{T}(\rho) = \frac{\int_0^{2\pi} \left(\iint_{\Sigma} U^*(\vec{r}, 0) \cdot U(\vec{r} + \vec{\rho}, 0) d^2\vec{r} \right) d\phi}{2\pi E_{\Sigma}} \quad (2)$$

The calculation of the field behind aperture in the framework of physical optics by means of $U(\vec{r}, 0)$ shall suppose the fulfillment of the following conditions:

- the inequation $\lambda/a \ll 1$ (a - is the aperture size): along with the condition of monochromatic radiation it enables to neglect edge effects on aperture, solve a scalar problem (in place of a vector problem) and pass on from the wave equation to the Helmholtz reduced wave equation $\Delta U(\vec{r}, z) + k^2 U(\vec{r}, z) = 0$, where $k = 2\pi/\lambda$, with boundary conditions of the Kirchhoff geometrical optics. In case of additional conditions of Sommerfeld's radiation

$$\lim_{r \rightarrow \infty} r(\partial U / \partial r - ikU) = 0$$

that provides the required rate of the field decay at infinity behind apertures, it has an exact integral solution to be solved by means of the Green function. For (1) we have taken the first Green function for plane apertures that gives the solution by means of the field on apertures without regard to the normal field derivative;

- the condition of paraxial zone $\vartheta \ll (\lambda/a)^{1/3}$: one may go over from the Helmholtz reduced wave equation to the parabolic equation $2ik(\partial U / \partial z) + \Delta_{x,y} U = 0$ ($\Delta_{x,y}$ - is the transverse Laplasian), the exact solution of which is called the Fresnel approximation;

- the condition for the wave parameter $D = \lambda z / \Sigma \gg 1$: it determines the z -distance from apertures (the diffraction Fraunhofer zone) where the Fresnel approximation is additionally simplified.

We shall further assume that the incident wave on apertures is plane. Then, without losing generality, the function $U(\vec{r}, 0)$ may be considered as real.

The optical transfer function (OTF) in uniform fields ($U(\vec{r}, 0) = const$) on apertures is equal to a overlapping area of two apertures displaced by ρ with respect to each other. The overlapping area is normalized to the aperture area, and $\bar{T}(\rho)$ - is the mean of the optical transfer function (OTF) with respect to the displacement angle. In other words OTF and $\bar{T}(\rho)$ are considered to be geometrical aperture characteristics. If the field is non-uniform, OTF and $\bar{T}(\rho)$ will be the field-averaged characteristics by $U(\vec{r}, 0)$. It follows from the equation (2) that $\bar{T}(0) = 1$.

When $\Delta_1 = 2\pi\vartheta\rho_1 / \lambda$ is close to zero, it follows from the equation (1) that

$$\varepsilon(\vartheta) \approx_{\Delta_1 \rightarrow 0} \pi \Sigma_{eff} \vartheta^2 / \lambda^2 = \frac{1}{4} \left(2\pi \frac{\rho_1}{\lambda} \vartheta \right)^2 \quad (3)$$

where the field-averaged aperture area is entered

$$\Sigma_{eff} = \frac{\left| \iint_{\Sigma} U(\vec{r}, 0) d^2 \vec{r} \right|^2}{E_{\Sigma}} = 2\pi \int_0^{\infty} \bar{T}(\rho) \rho d\rho \quad (4)$$

For the uniform field $\Sigma_{eff} = \Sigma$, and for the non-uniform field $\Sigma_{eff} \leq \Sigma$. The equation (3) defines the first characteristic length

$$\rho_1 = \sqrt{\Sigma_{eff}} / \pi \quad (5)$$

The paper [6] showed, from a series expansion of (1) according to Willis method [7], that the asymptotic approximation $\varepsilon(\vartheta)$ at larger $\Delta_2 = 2\pi\vartheta\rho_2 / \lambda$ is as follows

$$\varepsilon(\vartheta) \approx_{\Delta_2 \rightarrow \infty} 1 - \frac{(2/\pi)}{(2\pi\rho_2\vartheta/\lambda)} \quad (6)$$

where the second characteristic length - ρ_2 is determined as

$$\rho_2 = 2E_{\Sigma} / \int_c |U|^2 dl \quad (7)$$

The denominator in (7) has the integral over the aperture perimeter. In case of uniform fields the equation (7) goes over into the following:

$$\rho_2 = 2\Sigma / P \quad (8)$$

where P - is the aperture perimeter. The multipliers in (5,7) are taken so that for $U(\vec{r}, 0) = const$ on circular apertures $\rho_{1,2}$ are equal to circle radius. For uniform fields

$$\rho_2 = 2\Sigma / P \leq \sqrt{\Sigma / \pi} = \rho_1 \quad (9)$$

and the equation is true only for the circle. All the more, the equation (9) is true for non-uniform fields when a strict inequality has been performed even for the circle. So the equations (3) and (6) shall give the approximations (1) at smaller and larger values

$$\Delta_i = 2\pi\vartheta\rho_i / \lambda \quad (10)$$

In the interim $\varepsilon(\vartheta)$ may take different forms. There is the very few of analytical formulae for $\varepsilon(\vartheta)$ obtained. For example, the known Rayleigh function for circles at uniform fields may be written as follows

$$\varepsilon_{circ}(\Delta) = 1 - J_0^2(\Delta) - J_1^2(\Delta) \quad (11)$$

where $J_{0,1}(x)$ - means Bessel functions of orders 0 and 1. In (11) the parameter (10) has been taken without index because it includes the circle radius $\rho = \rho_{1,2}$. The approximations (3) and (6) properly describe (11) at smaller and larger Δ ; their combination connected at a cross point properly approximates the total Rayleigh function (see Fig. 2 in [2]).

The numerical calculation of the quadruple integral (1-2) due to oscillations J_1 takes considerable time, and it is required both in astronomy [8] and in some laser configurations [1]. The approximate calculation of (1) is assumed in many tasks. The paper [2] showed that in uniform fields and when parameter value

$$\mu = \rho_1 / \rho_2 \quad (12)$$

is close to 1 (in accordance to (9), $\mu \geq 1$) a fairly good approximation $\varepsilon(\vartheta)$ is (11) of Δ_2 (10) with ρ_2 from (8).

For the non-uniform field μ is larger than for the uniform field. When ρ_2 (7) is large (the field is small along the edges), then (6) shall “perform” only in proximity $\varepsilon(\vartheta) \approx 1$, and ρ_2 doesn’t already determine $\varepsilon(\vartheta)$ in intermediate domain.

For this situation the papers [2-3] presented that if the field on apertures varies smoothly (Gaussian or exponential functions), one may take (11) of the argument $\Delta_{2,eff} = 2\pi(\rho_{2,eff} / \lambda)\vartheta$, as the approximation $\varepsilon(\vartheta)$, where $\rho_{2,eff}$ is calculated as per (8) with Σ to be replaced by Σ_{eff} , and P – to be replaced by P_{eff} , obtained as a perimeter of a hole inside aperture equal in area to Σ_{eff} with a horizontal boundary of the field amplitude relief or along the aperture boundary (where it cuts off a contour line)

$$\rho_{2,eff} = 2\Sigma_{eff} / P_{eff} . \tag{13}$$

It also turned out that almost without loss of approximation accuracy one may not calculate P_{eff} for the hole equaled exactly to Σ_{eff} (in many cases it requires to solve transcendental equations), but may take the aperture area and perimeter, according to the same approach, which corresponds to the field amplitude $1/e^2$ of the maximum value (when the boundary field is greater, the aperture boundary should be considered).

The parameter (13) (and particularly its approximation “by level $1/e^2$ ”) is not followed from (1-2) and it is phenomenologically obtained. Its applicability has been proposed at $\varepsilon(\vartheta)$ for different apertures, including those in iodine photodissociation lasers with aperture fields of the Gaussian type or the exponent [1-2]. In [3] an unsuccessful effort was made to justify or improve a choice (13) for the approximation of the above type (11). Moreover, this approximation is completely poor, for example, if the field is large in a small part of the aperture (the “kernel”) and is small in its remaining, much greater, part (the “periphery”), and the energies in the “kernel” and the “periphery” are comparable.

We have proposed here a different, other than in [2-3], method of approximation $\varepsilon(\vartheta)$ based on the models $\bar{T}(\rho)$. If $F(y)$ – is the integral transformation $f(x)$ with an oscillatory core $G_{osc}(xy)$ (as per (1))

$$F(y) = \int G_{osc}(xy) \cdot f(x)dx \tag{14}$$

the oscillations G_{osc} may smooth over a contribution of f into F .

As a matter of fact, $F(y)$ defines not a proper type of $f(x)$, but a set of its numerical characteristics (invariants). Then the model $f(x)$, even not simulating it properly but retaining these invariants, can provide good approximation of $F(y)$ which depends on the invariants.

This determination was obtained in [9-10] as a result of numerical experiments with the calculation of statistical characteristics of the narrow-band random pro-

cess that has induced the similar approach to the approximation $\varepsilon(\vartheta)$, because the integral (1) is similar to (14) in its structure. Since both the kernels $G_{osc}(xy)$ in (1) are different and $f(x)$ has also a different meaning, the approach was not so much mathematical as physical, i.e. the choice of necessary invariants was made due to the physical sense of $f(x)$.

In [9-10] $f(0)$ and $G_{osc}(0)$ in (14) are equal to absolute maxima, i.e. the oscillations G_{osc} cut off a tail of $f(x)$. In (1) $\bar{T}(0)$ – is the maximum, but $J_1(0) = 0$, thus it does not cut off the tail but the maximum $\bar{T}(\rho)$. Therefore for the approximation $\varepsilon(\vartheta)$ according to the method presented in [9-10] the formula (1) was converted based on Bessel function properties by means of by-part integrating as follows

$$\varepsilon(\vartheta) = 1 - \int_0^\infty \Gamma(\rho) J_0\left(\frac{2\pi\vartheta}{\lambda}\rho\right) d\rho \tag{15}$$

where $J_0(x)$ – is the zero-order Bessel function with already desired type of kernel (14) (the maximum is at zero and decrease is performed with increasing the argument), and $\Gamma(\rho)$ is determined as follows

$$\Gamma(\rho) = -\bar{T}'(\rho) . \tag{16}$$

When (15) deduced from (1), the equations $J_0(0) = 1$; $\bar{T}(0) = 1$; $\bar{T}(\infty) = 0$.

(17) shall be taken into consideration. The numerical calculation of $\varepsilon(\vartheta)$ (if $\Gamma(\rho)$ are analytically unknown) was performed not according to (15) but according to (1), since otherwise the calculation of the triple integral (2) is to be added by one more task of the numerical calculation of the derivative $\bar{T}(\rho)$.

The function $\Gamma(\rho)$ shall meet the following conditions:

$$\Gamma(0) = \frac{2}{\pi\rho_2}; \int_0^\infty \Gamma(\rho) d\rho = 1; \int_0^\infty \Gamma(\rho)\rho^2 d\rho = \frac{\Sigma_{eff}}{\pi} \tag{18}$$

The third equation in (18) arises from (4), the second – from (16-17), and the first – from the equation $\bar{T}'(0) = -2 / \pi\rho_2$ obtained in [6] for uniform fields on aperture and generalized in [2] for non-uniform fields (see (6)).

It follows from (16-17) the relationship of moments of $\Gamma(\rho)$ and $\bar{T}(\rho)$

$$\int_0^\infty \Gamma(\rho)\rho^n d\rho = n \int_0^\infty \bar{T}(\rho)\rho^{n-1} d\rho \tag{19}$$

Let’s first consider the case of uniform fields on apertures when many characteristics have got a clear geometric interpretation.

2. Uniform fields on apertures

Let us enter, for convenience in place of (16), the dimensionless function $\tilde{\Gamma}(\zeta)$ of the dimensionless argument

$$\tilde{\Gamma}(\zeta) = \frac{\pi\rho_2}{2} \Gamma(\rho = \rho_2\zeta) = -\frac{\pi}{2} \bar{T}'_\zeta(\rho = \rho_2\zeta) \quad (20)$$

where $\zeta = \rho/\rho_2$, ρ_2 is set in (8). The equations (18) shall go over into

$$\tilde{\Gamma}(0) = 1; \int_0^\infty \tilde{\Gamma}(\zeta) d\zeta = \pi/2; \int_0^\infty \tilde{\Gamma}(\zeta) \zeta^2 d\zeta = \mu^2 \pi/2 \quad (21)$$

and the expression (15), by means of Δ_2 , shall go from (10) into

$$\varepsilon(\Delta_2) = 1 - \frac{2}{\pi} \int_0^\infty \tilde{\Gamma}(\zeta) J_0(\Delta_2 \zeta) d\zeta. \quad (22)$$

If μ (12) is known and the model $\tilde{\Gamma}_{\text{mod}}(\zeta)$ that satisfies (21) is to be substituted to (22), the obtained function $\varepsilon_{\text{mod}}(\Delta_2)$ with exact $\varepsilon(\Delta_2)$ shall have equal behaviors $(\Delta_2 \mu/2)^2$ (3) in the origin of the angle coordinates and asymptotics $1 - (2/\pi)/\Delta_2$ (6) at infinity. The function $\varepsilon(\Delta_2)$ does not decrease, tends to unity and can have flex points (the Fraunhofer dark rings on a diffraction pattern). If in graph with Δ_2 x-axis we draw two functions (11) of $\Delta_1 = \mu\Delta_2$ and Δ_2 , then $\varepsilon(\Delta_2)$ shall first go along the first curve, and in the end it shall go over into the second curve. The transition may be diverse, i.e. monotone, with flex points or with a nearly lateral jump-over in the neighborhood of a top “plateau”. Fig. 1 shows four functions (20) for different aperture shapes with $\mu = 1,7$ (rectangle, ring and two toothed apertures (TA)) taken from [2] and defining diverse functions $\varepsilon(\Delta_2)$ (see Fig. 2). The toothed apertures (TA) are the gears with gear teeth in the form of ring pieces cut off radially. The shape of toothed apertures possesses a symmetry axis of the n -order and is determined by three parameters, i.e. the relationship of concentric circle radiuses d , a number of equal teeth n and the ring-teeth-filling factor η (a part of the ring occupied with teeth).

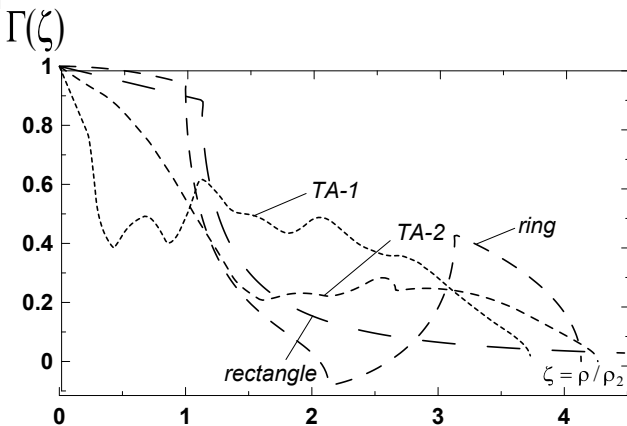


Fig.1. Functions $\tilde{\Gamma}(\zeta)$ for four different apertures with $\mu = \rho_1/\rho_2 = 1,7$: TA-1; TA-2; the ring; the rectangle (the curve line extends to $\zeta = 8,8$);

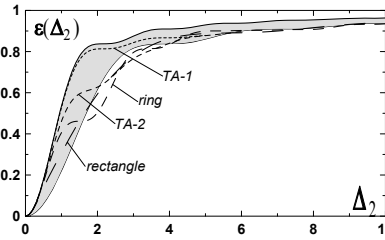


Fig.2. Functions $\varepsilon(\Delta_2)$ are dashed-line curves corresponding to $\tilde{\Gamma}(\zeta)$ in Fig. 1. Full lines show the functions (11) of parameters $\mu\Delta_2$ (left) and Δ_2 (right); the area between them is painted over

For the numeric calculation of $\tilde{\Gamma}(\zeta)$ for TA, proper software has been developed which was also used for $\tilde{\Gamma}(\zeta)$ of ring apertures with non-uniform fields. From the obtained sets (d, n, η) for $\tilde{\Gamma}(\zeta)$ Fig. 1 we have selected two ones, where $\mu = 1,7$: TA-1 (0.77; 10; 0.75) and TA-2 (0.25; 3; 2/3). In the rectangle $\mu = 1,7$ is equal to $a/b = 9,84$ ($\mu = (a+b)/\sqrt{\pi ab} \in [2/\sqrt{\pi} \approx 1,13; \infty)$), and in the ring it is equal to the ratio $d = 0,52$

$$(\mu = \sqrt{(1+d)(1-d)} \in [1; \infty)).$$

For the ring and the rectangular $\tilde{\Gamma}(\zeta)$ are handled analytically [11-13]. We shall need $\tilde{\Gamma}(\zeta)$ for the ring

$$\tilde{\Gamma}_{\text{ring}}(\zeta) = \frac{\sqrt{(\mu^2+1)^2 - \zeta^2}, \zeta \leq \mu^2+1}{2\mu^2} + \frac{\sqrt{(\mu^2-1)^2 - \zeta^2}, \zeta \leq \mu^2-1}{2\mu^2} - \frac{\sqrt{\mu^4 - \zeta^2} \sqrt{\zeta^2 - 1}/\zeta, 1 \leq \zeta \leq \mu^2}{\mu^2} \quad (23)$$

For the approximation $\varepsilon(\Delta_2)$ we tested a number of models $\tilde{\Gamma}(\zeta)$ selected based on three considerations, i.e. the possibility of analytical calculation (22) with $\tilde{\Gamma}_{\text{mod}}(\zeta)$ (or by means of the integral of parameters which may be tabulated); simplicity in the calculation of model parameters by means of characteristics of apertures, the field or $\bar{T}(\zeta)$; and model usability for the non-uniform field on apertures.

There are not so many analytically integrable functions in (22). In $\tilde{\Gamma}_{\text{mod}}(\zeta)$ we have used the linear function ((22) together with it provide Bessel and Struve functions),

$$f(x) = \sqrt{k^2 - x^2} \quad (24)$$

of the type of $\tilde{\Gamma}_{\text{circ}}(\zeta) = \sqrt{1 - (\zeta/2)^2}$ of the circular aperture and two first summands in (23) ((22) of (24) on the interval $[0, k]$ gives (11)) and the function of the third summand in (23)

$$f(x) = \sqrt{k^2 - x^2} \sqrt{x^2 - 1} / x \quad (25)$$

The integral (22) of (25) on the interval $[1, k]$ is not analytically calculated and it depends on k and one more parameter.

The given models $\tilde{\Gamma}_{\text{mod}}(\zeta)$ possess the parameters. In [11-13] several models have been considered possessing a number of 1 to 3 free parameters (after the execution of (21)) and different sources for these parameters. This paper presents some results of this analysis and shows the best models with the most successful selection of free parameters.

The first group $\tilde{\Gamma}_{\text{mod}}(\zeta)$ represents piecewise linear models with 1-3 free parameters. Their analysis for the examples in Fig. 1 has shown that the close approximation $\varepsilon(\Delta_2)$ is provided by one-parametric rectangle and triangle models $\tilde{\Gamma}_{\text{mod}}^{\text{rec,tri}}(\zeta)$, regardless of roughness of the approximation $\tilde{\Gamma}(\zeta)$ (Fig. 3).

Their parameters are calculated from quadratic equations (see below). The models with greater number of free parameters “fail” to the models in Fig. 3 for several reasons, i.e. the equations become more complicated to calculate the parameters from the values of aperture invariant characteristics; more characteristics are needed; it often happens that the calculated parameters cannot meet all necessary requirements. This is also true for non-uniform fields on apertures.

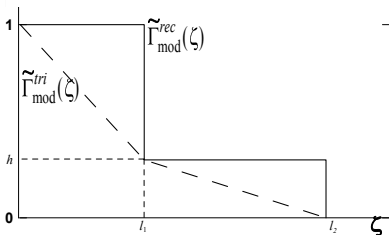


Fig.3. One-parameter models $\tilde{\Gamma}_{\text{mod}}^{\text{rec,tri}}(\zeta)$. The value of $\tilde{\Gamma}_{\text{mod}}(0)$ and two of three parameters on the graph are determined by the equations (21), one parameter is free. In the context thereof $0 < l_1 \leq l_2$, and h – may be of any value

Of course, the more parameters, the greater approximation opportunities. However the aforementioned limitations bring these advantages to naught. Performance potentials of the models in Fig. 3 (using manual selection of free parameters) allow one to better improve the approximation $\varepsilon(\Delta_2)$. Improvements occurred due to model complications are negligible for considered sources of parameters and they even can't always be observed.

It is convenient to calculate model parameters in Fig. 3 by means of

$$a = l_1 + l_2 \tag{26}$$

assuming this to be a free parameter. Then for the model $\tilde{\Gamma}_{\text{mod}}^{\text{tri}}(\zeta)$ in Fig. 3 we shall have the following from the equations (21)

$$b = l_1 l_2 = \frac{\pi + a}{\pi + a - 6\mu^2}; \quad h = \frac{\pi - l_1}{l_2} \tag{27}$$

For existing real positive values l_1, l_2 in (26-27) it is necessary and sufficient that a shall meet the following requirement (provided $\mu \geq \pi / \sqrt{6} \approx 1,28$) [12-13]

$$a > \mu\sqrt{6} \tag{28}$$

Provided $1 \leq \mu < \pi / \sqrt{6}$, the requirement for a is different (see [12-13]), but $\mu \approx 1,28$ is small even for uniform fields, and all examples herein shall refer to the case when $\mu \geq 1,28$. The value $\mu\sqrt{6}$ in table below is called a_{min} .

The parameter a (26) may be taken from different aperture characteristics. Let us consider some opportunities [11-13]. For example, it may be taken from unengaged in (21) moments of $\tilde{\Gamma}(\zeta)$ (i.e. $\tilde{T}(\zeta)$ – see (19)), i.e.

$$I_1 = \int_0^\infty \tilde{\Gamma}(\zeta)\zeta d\zeta; \quad I_3 = \int_0^\infty \tilde{\Gamma}(\zeta)\zeta^3 d\zeta; \quad I_4 = \int_0^\infty \tilde{\Gamma}(\zeta)\zeta^4 d\zeta \tag{29}$$

The values I_1 for considered apertures are given in the table below, and $I_{3,4}$ – in [11, 13]. Using the moment I_1 the parameter (26) for $\tilde{\Gamma}_{\text{mod}}^{\text{tri}}(\zeta)$ in Fig. 3 shall be calculated by

$$a_{I_1} = 6\pi(\mu^2 - I_1) / (6I_1 - \pi^2) \tag{30}$$

Though (30) is quite favorable for the apertures and fields analyzed, let's also consider some other options (26).

If in (15) we expand $J_0(x)$ in a zero Taylor series up to x^4 , the following member shall be added to (3)

$$\varepsilon(\Delta_2) \approx (\Delta_2^2 \mu^2 / 4) - (\Delta_2^4 / 32\pi) I_4 \tag{31}$$

i.e. I_4 may also be obtained as a source for (26). In accordance to (31), this should improve the approximation $\varepsilon(\Delta_2)$ in the origin of the angle coordinates, but this correction is low-observable. Replacing a_{I_1} by a_{I_4} don't improve the approximation $\varepsilon(\Delta_2)$, although these two options are close to each other. Using I_4 for $\tilde{\Gamma}_{\text{mod}}^{\text{tri}}(\zeta)$ the parameter a_{I_4} is calculated from the 4th-degree equation

$$a^4 - (6\mu^2 + A)a^2 - 2\pi Aa - A\pi^2 = 0 \tag{32}$$

where $A = [6(5I_4 - 6\pi\mu^4)] / [(6\mu^2 - \pi^2)\pi]$, and it should meet the above requirements (28).

One can also obtain a from the condition that $l_2 = \zeta_{\text{max}}$, where ζ_{max} – is the maximum ζ , for which $\tilde{\Gamma}(\zeta) \neq 0$ (and $T(\zeta) \neq 0$).

It equals to $a_\zeta = (\zeta_{\text{max}} + \sqrt{\zeta_{\text{max}}^2 + D}) / 2$,

where $D = 4\pi(\zeta_{\text{max}}^2 - 6\mu^2) / (\zeta_{\text{max}} - \pi)$.

For the fulfillment of $a_\zeta \geq l_2$ we need $D \geq 0$.

Along with (28) it may restrict ζ_{max} :

$$\begin{cases} \zeta_{\text{max}} \geq \sqrt{6}\mu \\ 0 < \zeta_{\text{max}} < \pi \end{cases} \tag{33}$$

where, as in (28), it is assumed that $\mu \geq \pi / \sqrt{6}$. See a contrary option in [13].

The values ζ_{max} and a_ζ of the considered examples are also given in the table below. The requirements of (33) from apertures in Fig. 1 may be satisfied only by the rectangle.

Table. Characteristics $\tilde{\Gamma}(\zeta)$ for seven apertures and the fields thereon and different values of a (26) for the triangle model in Fig. 3 (dashes mean that the parameter does not exist or not meet the requirement (28))

	μ	I_1	ζ_{\max}	\mathfrak{a}	a_{\min}	a_{I_1}	a_{I_4}	a_ζ	$a_{\mathfrak{a}}$	a_{\approx}
Rectangle $a/b=9,84$	1.77	1.85	8.77	0.10	4.34	19.5	12.9	11.6	-	13-15
Ring $d=0,2$	1.77	2.00	4.13	0	4.34	10.2	7.36	-	-	7-9
TA-1	1.77	2.32	3.74	1.02	4.34	-	-	-	4.78	4.3-4.7
TA-2	1.77	2.12	4.27	0.31	4.34	6.62	5.91	-	-	6.5-7
Example 1	3.37	3.61	20.8	0.75	8.25	12.4	12.1	23.6	10.5	12-13
Example 2	5.34	4.35	17.9	0.77	13.1	28.0	28.7	19.5	16.9	20-22
Example 3	12.0	10.1	34.3	-	29.5	50.4	63.4	35.2	<0	39-40

For $\tilde{\Gamma}_{\text{mod}}^{\text{tri}}(\zeta)$ the parameter (26) may also be obtained from a zero slope ratio $\tilde{\Gamma}(\zeta) \approx 1 - \mathfrak{a}\zeta + \dots$ $\zeta \rightarrow 0$

$$\mathfrak{a} = -\tilde{\Gamma}'_{\zeta}(0) = (\pi/2) \cdot \bar{T}'_{\zeta}(0). \tag{34}$$

Using (34) $a_{\mathfrak{a}} = \sqrt{\pi(6\mu^2\mathfrak{a} - \pi) / (\pi\mathfrak{a} - 1)}$. The series obtained for (22) in [7] (and more thoroughly analyzed in [14]) is presented only by the even derivatives $\tilde{\Gamma}(\zeta)$ and doesn't contain (34):

$$\varepsilon(\Delta_2) \approx 1 - \frac{2}{\pi\Delta_2} + \frac{\tilde{\Gamma}''_{\zeta}(0)}{\pi\Delta_2^3} + \dots \tag{35}$$

In (35) only two first members are the asymptotic expansion (22) at infinity (vs (6)) and there is no summand of the type Δ_2^{-2} , as, for example, in asymptotics (11) [15]

$$\varepsilon_{\text{circ}}(\Delta) \approx 1 - \frac{2}{\pi\Delta} + \frac{\cos 2\Delta}{\pi\Delta^2} - \frac{1 - \sin 2\Delta}{4\pi\Delta^3} + \dots$$

There is no any formula for the calculation of \mathfrak{a} in arbitrary case. According to [3], the field non-uniformity provides contributions only into the zero even derivatives $\bar{T}(\zeta)$ (i.e. into the odd derivatives $\tilde{\Gamma}(\zeta)$). With regard to $\bar{T}'(0)$ from [2,6] and a part of $\bar{T}''(0)$ of non-uniformities we shall obtain the following [12-13]

$$\bar{T}(\zeta) \approx 1 - \zeta \frac{2}{\pi} + \tag{36}$$

$$+\zeta^2 \frac{\rho_2^2 \cdot \iint_{\Sigma} U^* \cdot \nabla_{\perp} U d^2\vec{r}}{4E_{\Sigma}} + \dots$$

In (36) in the general case the coefficient at ζ^2 (presetting \mathfrak{a}) is not total, i.e. there is a contribution of the field non-uniformity therein and no contribution of the aperture boundary. However, for the examples considered in this paper \mathfrak{a} is to be calculated. At uniform fields for apertures in Fig. 1: $\mathfrak{a}_{\text{rec}} = 1/(\pi\mu^2)$;

$$\mathfrak{a}_{\text{TA}} = \frac{n(1-\eta + d^2\eta)}{\pi[1-\eta + d\eta + n(1-d)/\pi]^2}.$$

$\mathfrak{a}_{\text{ring}} = 0$ And even at equal μ they differ greatly. And in the non-uniform field for three examples considered below, due to the radial symmetry of fields and apertures, \mathfrak{a} is just provided with the third summand (36), i.e.

$$\mathfrak{a} = \pi E_{\Sigma} \iint_{\Sigma} U^* \cdot \nabla_{\perp} U d^2\vec{r} / (\oint_C |U|^2 dl)^2$$

Thus \mathfrak{a} and $a_{\mathfrak{a}}$ are also given in the above table. In Fig. 1 only for TA-1 there exists $\tilde{\Gamma}_{\text{mod}}^{\text{tri}}(\zeta)$ by \mathfrak{a} (the requirement (28) hasn't been fulfilled for the rectangle and the ring, and for TA-2 $a_{\mathfrak{a}}$ has an imaginary value).

From (22) $\varepsilon_{\text{mod}}^{\text{tri}}(\Delta_2)$ for $\tilde{\Gamma}_{\text{mod}}^{\text{tri}}(\zeta)$ in Fig. 3 equals to

$$\varepsilon_{\text{mod}}^{\text{tri}}(\Delta_2) = 1 - 2/[\pi(l_2 - l_1)] \times \left[\frac{l_1((1-h)l_2 - l_1)F(l_1\Delta_2) + l_2^2 hF(l_2\Delta_2) - ((1-h)l_2 - l_1)J_1(l_1\Delta_2) + l_2 hJ_1(l_2\Delta_2)}{\Delta_2} \right] \tag{37}$$

where $F(x) = J_0(x) + (\pi/2)(J_1(x)H_0(x) - J_0(x)H_1(x))$; whereas J_i and H_i - are the i -order Bessel and Struve functions.

The expressions similar to (27-28,30,32-33,37) in their structure are also obtained for the rectangle model $\tilde{\Gamma}_{\text{mod}}^{\text{rec}}(\zeta)$ (Fig. 3). They are presented in [13].

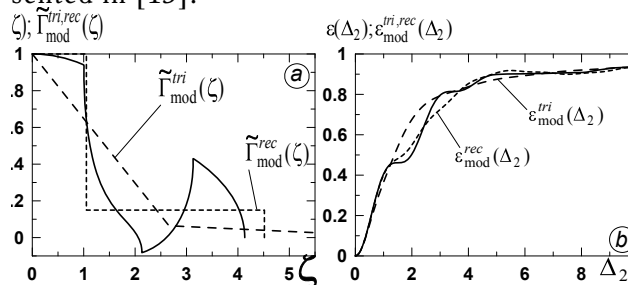


Fig. 4. For the ring aperture with $\mu_{\approx}=1,7$: (a) - the graphs of $\tilde{\Gamma}(\zeta)$ (full line) and the models $\tilde{\Gamma}_{\text{mod}}^{\text{tri,rec}}(\zeta)$ Fig. 3 (dashed lines) at $a = a_{I_1}$. For $\tilde{\Gamma}_{\text{mod}}^{\text{tri}}(\zeta)$ the tail is cut-off on the graph; (b) - the graphs of $\varepsilon(\Delta_2)$ and $\varepsilon_{\text{mod}}^{\text{tri,rec}}(\Delta_2)$ for $\tilde{\Gamma}_{\text{mod}}^{\text{tri,rec}}(\zeta)$ from (a) (line types are matched)

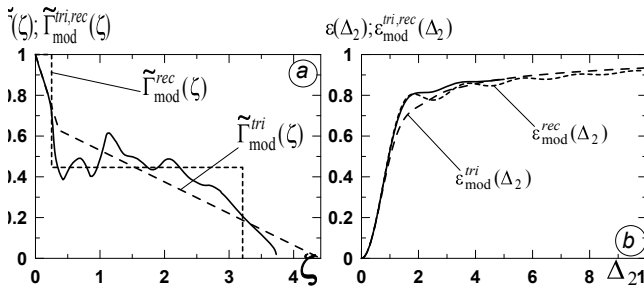


Fig.5. For TA-1 with $\mu = 1,7$: (a) - the graphs of $\tilde{\Gamma}(\zeta)$ (full line) and the models $\tilde{\Gamma}_{\text{mod}}^{\text{rec}}(\zeta)$ at $a = a_{I_1}$, $\tilde{\Gamma}_{\text{mod}}^{\text{tri}}(\zeta)$ at $a = a_x$ (dashed lines); (b) - the graphs of $\varepsilon(\Delta_2)$ and $\varepsilon_{\text{mod}}^{\text{tri,rec}}(\Delta_2)$ for $\tilde{\Gamma}_{\text{mod}}^{\text{tri,rec}}(\zeta)$ from (a) (line types are matched)

The calculation of $\varepsilon_{\text{mod}}^{\text{tri,rec}}(\Delta_2)$ for apertures in Fig. 1 at a from the above table has shown [11-13] that both models can simulate $\varepsilon(\Delta_2)$ well and similar in accuracy, however $\varepsilon_{\text{mod}}^{\text{tri}}(\Delta_2)$ is more preferred, because (37) is usually monotonic as $\varepsilon(\Delta_2)$, and $\varepsilon_{\text{mod}}^{\text{rec}}(\Delta_2)$ has detectable local extreme points. To estimate how well (37) can approximate the exact $\varepsilon(\Delta_2)$, (26) was also selected manually for the better approximation $\varepsilon(\Delta_2)$ (a_{\sim} in the above table). At a_{I_1} - (37) differed from $\varepsilon(\Delta_2)$ in the whole range of Δ_2 within 10-15%. Figs. 4-5 show two worse examples, i.e. for the ring aperture and TA-1.

In [11-13] one more model of $\tilde{\Gamma}(\zeta)$ was considered based on (23) for the ring apertures, i.e. $\tilde{\Gamma}_{\text{mod}}^r(\zeta)$. In (23) the coefficients are determined by μ (12), they were assumed to be of any kinds in the model (each summand is taken on the interval where it is real):

$$\tilde{\Gamma}_{\text{mod}}^r(\zeta) = \alpha\sqrt{a^2 - \zeta^2} + \beta\sqrt{b^2 - \zeta^2} + \gamma\sqrt{c^2 - \zeta^2}\sqrt{\zeta^2 - g^2} / \zeta \quad (38)$$

In (38) there are seven parameters limited in sense: $0 < a \leq b; 0 < g < c; c < b; \alpha, \beta > 0$ (39)

where the relationship of a and b was taken for definiteness; the second inequality is obvious; and the last two ones give a typical type of $\tilde{\Gamma}(\zeta)$ and $\varepsilon(\Delta_2)$. Perhaps, the condition $\alpha, \beta > 0$ in (39) may be eliminated just as it was done with the requirement $\gamma \leq 0$ corresponding to (23). However, since even with (39) some good solutions have been found for all examples, the options not acceptable by (39) were rejected.

Taking into account (21), there are four free parameters left in (38). Their search by means of I_i (29) shall result to the system, where in odd-moment conservation equations for $\tilde{\Gamma}_{\text{mod}}^r(\zeta)$ the ratio of unknown variables g/c is included into the arguments of elliptic integrals. To avoid this, the model (38-39) was simplified by superposition of the relationship of g and c , as in (23) $p = g/c = 1/\mu^2$ (40)

Then elliptic integrals depending on p in conservation equations for $I_{1,3}$ became numerical coefficients

in the system of algebraic equations for the rest of three parameters. For the apertures in Fig. 1 at least two or three real solutions for model (38-40) have been obtained by means of $I_{1,3,4}$, even for the ring apertures. All of them, regardless of the difference in respective functions (38), have given close and good approximations $\varepsilon(\Delta_2)$ (better than the models in Fig. 3 – see [11]). Most of these solutions roughly met the requirements of one of two equations (which is not the case in (23))

$$c = a \quad (41)$$

$$c = b \quad (42)$$

Therefore in [11] we have considered the model (38-41), and in [13] – the model (38-40,42) (two free parameters have been taken from the moments $I_{1,3}$). As well as two one-parameter models (38-40) ($b = \zeta_{\text{max}}$, one of the requirements (41-42) has been fulfilled, and the resting parameter was taken from I_1). For all apertures in Fig. 1 these one- and two-parameter models possessed one or two solutions each and provided close and good approximations $\varepsilon(\Delta_2)$; besides, the accuracy of their approximation seemed to be better than for a three-parameter model (38-40). Even for the ring apertures, the exact function (23) of which can satisfy neither (41) nor (42) (see Fig. 6). By means of manual selection of parameters for these models (not by means of I_i) we nearly managed to obtain the coincidence of $\varepsilon_{\text{mod}}^r(\Delta_2)$ with $\varepsilon(\Delta_2)$.

The function $\varepsilon_{\text{mod}}^r(\Delta_2)$ consists of two functions (11) (obtained from the first two summands in (38)) and the two-parameter integral of the function (25) (from the third summand in (38)).

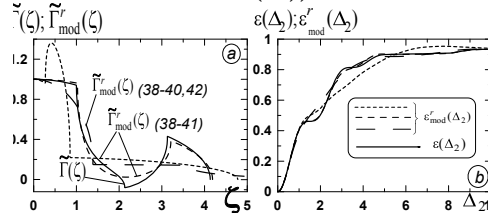


Fig.6. For the ring aperture with $\mu = 1,7$: (a) - the graphs of $\tilde{\Gamma}(\zeta)$ (full line) and the two-parameter models $\tilde{\Gamma}_{\text{mod}}^r(\zeta)$ (38-41) (short and medium dashes) and (38-40,42) (long dashes, tail cut-off) with free parameters from $I_{1,3}$; (b) - the graphs of $\varepsilon(\Delta_2)$ and $\varepsilon_{\text{mod}}^r(\Delta_2)$ for $\tilde{\Gamma}_{\text{mod}}^r(\zeta)$ from (a) (line types are matched)

Fig. 6 shows an example of approximation $\varepsilon(\Delta_2)$ by the function $\varepsilon_{\text{mod}}^r(\Delta_2)$ of two-parameter models (38-41) and (38-40,42) with parameters from $I_{1,3}$.

One of the approximations here is supposed to be the worst among all such approximations for apertures in Fig. 1. However, its relative error has never exceeded 15%.

3. Spatially-nonuniform fields on apertures

For non-uniform fields on apertures μ (12) is increased and the functions (11) of Δ_2 and $\mu\Delta_2$ are more dispersed (vs Fig. 2), and there is no information about $\varepsilon(\Delta_2)$ in intermediate domain. In this case the proposed in [2-3] approximation $\varepsilon(\Delta_2)$, by means of the function (11) with some phenomenological argument normalization (the calculation of which is considered to be a separate problem), coincides neither with (3) at small, nor with (6) at large values of the argument, and it may be applied only for smooth fields on apertures of the Gaussian type or the exponent.

Let us use here the aforesaid models. We shall be restricted to the ring apertures and three examples of fields for which the approach [2-3] gives bad approximation. The fields descend radially and possess a radial symmetry like apertures.

Example 1. The radius ratio is $d = 0,2$; the field exponentially descends from the inner radius r_1 into the outer radius r_2 by $e^{10} \approx 2,2 \cdot 10^4$ times.

Example 2. The radius ratio is $d = 0,7$; the field exponentially descends from the outer radius r_2 into the inner radius r_1 by $e^{2,5} \approx 12,2$ times.

Example 3. The radius ratio is $d = 0,5$; the field descends from r_1 into r_2 in accordance with the law

$$U(x = \frac{r}{r_2}) = \begin{cases} \sqrt{1-32(x-d)}, d \leq r \leq d^* \\ \delta = \sqrt{1-32(d^*-d)} = \sqrt{0,02}, d^* \leq r \leq 1 \end{cases},$$

i.e. there is a narrow “ring-kern” ($d^* = 0,53125$) where U^2 drops down linearly, and the “periphery” where the field is constant, and the energies E_1 in the “kern” and E_2 in the “periphery” are close to each other, i.e. $E_1 / E_2 \approx 1,11$. The number $\delta^2 = 0,02$ is close to $e^{-4} \approx 0,018$, which in [2-3] estimates the level U^2 of aperture efficient boundary for non-uniform fields. The approximation in [2-3] was the worst for these fields.

Characteristics of Γ for **examples 1-3** and parameters of their models $\tilde{\Gamma}_{mod}^{tri}$ in Fig. 3 are given in the above table and in [11-13]. Comparison for **examples 1-3** $\varepsilon_{mod}^{tri,rec}$ with exact ε [11-13] has shown that here also ε_{mod}^{tri} is better than ε_{mod}^{rec} and it is quite acceptable at $a = a_{I_1}$.

Slightly inferior to it are (37) with $a = a_{I_4}, a_\zeta$, which are worse with $a = a_{\infty}$ (a slope $\Gamma(0)$ is not important in simulation of ε) – see Fig. 7 for the **examples 2-3** at all a -values from the above table (the **example 1** presents higher approximation accuracy).

Functional arguments in Fig. 7 and Fig. 8 are normalized not on (7) as in Fig. 1-2,4-6, but on (13) as in [2-3, 11-13].

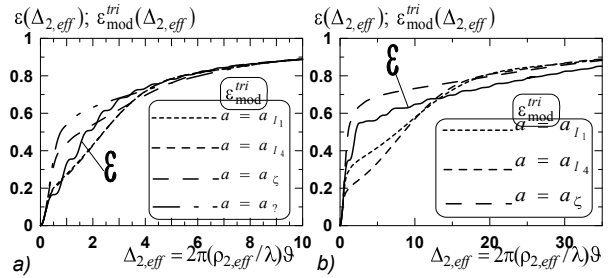


Fig.7. The graphs of exact ε and ε_{mod}^{tri} (37) with parameters from the above table for **example 2** (a) and **example 3** (no curve line with $a = a_{\infty}$) (b)

Calculations of ε_{mod}^r for **examples 1-3** (models of the “ring” $\tilde{\Gamma}_{mod}^r$) have shown that three-parameter models (using moments $I_{1,3,4}$) are not successful, i.e. there were always two or four unequal options most of which were non-monotone. One-parameter models by I_1 are missing for all **examples 1-3** both at (41) and at (42). However, there exist two-parameter models by $I_{1,3}$ in one or two options both at (41) and at (42), and they are close in quality to ε_{mod}^{tri} (37). The paper [11] gives their parameters and graphs at (41), and the paper [13] – at (42). The approximations at (42) proved to be better than at (41), and for **examples 1-2** they are more exact than for **example 3**. Fig. 8 gives three available options for **example 3**: one at (41) (the worst) and two at (42), one of which is very close to the ideal. Two-parameter models (38-40,41) and (38-40,42) can assume a great variety of functions $\tilde{\Gamma}_{mod}^r$.

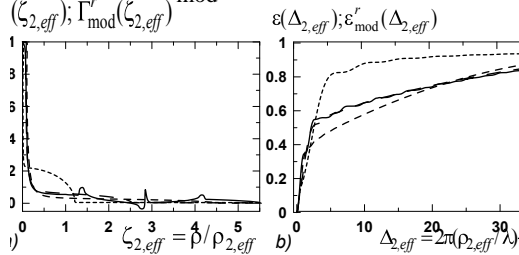


Fig.8. For **example 3**: (a) – the graphs of exact $\tilde{\Gamma}$ (full line) and two-parameter models $\tilde{\Gamma}_{mod}^r$ (38-40) (dashed lines, tails cut-off): one curve line is at $C = a$ (short dashes) and two curve lines – at $C = b$ (medium and long dashes); (b) – the graphs of exact ε and ε_{mod}^r for $\tilde{\Gamma}_{mod}^r$ from (a) (line types are matched)

So, for plane fields on apertures the one-parameter triangle model (37) and the two-parameter model of the “ring” ε_{mod} at (39-40,42) can both provide good approximations $\varepsilon(\Delta)$, if we take the moments $\tilde{\Gamma}$ for the calculation of missed parameters.

The paper excludes the cases with “soft” apertures defined only by the field, without a screen; they are poorly described by the offered approach. The parameter (7) shall become infinite then and cannot be used in (12,18,20-21). From (6), in place of the first equation (18), it follows that $\Gamma(0) = 0$, i.e. individuality of $\Gamma(0)$ is missing, which means that behavior specificity of ε at large values of the argument is missing, too.

Calculations of $\varepsilon(\Delta)$ given in [13] for such radially non-symmetrical fields, descending in phase uniformity plane from the centre according to the Gaussian or the exponent laws with different coefficients in perpendicular axes, have shown that at equal I_1 the functions $\varepsilon(\Delta)$ may vary notably, i.e. generally they can't be approximated by models with I_1 as the source of the missing model parameter.

Conclusion

The function $\varepsilon(\vartheta)$ is the integral transformation of $\Gamma(\rho)$ (16), the derivative of $\bar{T}(\rho)$, reversed in sign, with a kernel in the form of the zero-order Bessel function. In proximity to zero, $\varepsilon(\vartheta)$ is determined by the second moment $\Gamma(\rho)$ (3), and at larger values of the argument [2, 6] – by the value $\Gamma(0)$ (6) (see (18)). These both characteristics of $\Gamma(\rho)$ are defined by aperture geometry, i.e. by its area and perimeter averaged in accordance with field distribution on apertures; and simply by its area and perimeter – for uniform fields. However it is not sufficient for presentation of $\varepsilon(\vartheta)$ within the whole range of determination. Such as areas and perimeters (with or without averaging) cannot reflect diversity of apertures and fields thereon.

By assuming that $\varepsilon(\vartheta)$ between (3) and (6) is mainly determined by one or two more characteristics of apertures and fields thereon, we have succeeded in obtaining good approximations for $\varepsilon(\vartheta)$ by means of replacement of $\Gamma(\rho)$ with the models meeting the above requirements (18) and maintaining these additional characteristics.

Let us take moments of $\Gamma(\rho)$ or ρ_{\max} (if μ (12) is not large) in place of the latest, and linear functions and the functions included into $\Gamma(\rho)$ of ring apertures for uniform field – as the model $\Gamma(\rho)$. Therefore for the approximation $\varepsilon(\vartheta)$ with the relative accuracy of 10-15% it would be enough to involve one or two moments $I_{1,3}$. The calculation of their larger quantity shall not improve the accuracy of approximation thus deteriorating it upon other indications, i.e. there are no solutions on model parameters available, $\varepsilon_{\text{mod}}(\Delta)$ has acquired “non-physical” local extreme points, etc. It is typical that the

good approximation $\varepsilon(\vartheta)$ doesn't require the same from the model $\Gamma(\rho)$ which is supposed to be only a “carrier” of invariant characteristics.

Beyond the analysis we have left the feasibility of selection of I_n and ρ_{\max} as additional invariant characteristics of apertures and the field thereon.

References

1. Borovich BL, Zuev VS, Katulin VA., Mikheev LD, Nikolaev FA, Nosach OYu, Rozanov VB. High-current emitting discharges and optically pumped gas lasers [In Russian]. Moscow: VINITI Publisher “Progress in Science and Technology, Radio Engineering Series”; 1978: 15.
2. Sizova IM. Approximate scaling relationships of light diffraction by apertures with complicated shapes. *Appl Optics* 1992; 31(28): 5930-6.
3. Sizova IM. Similarity diffracted in the far field by apertures of complicated shape. *J of Sov Laser Res* 1992; 13(1): 25-45.
4. Born M, Wolf E. Principles of Optics. New York: Macmillan; 1959.
5. Piatakhin MV, Suchkov AF. Plane electromagnetic wave diffraction by the circular diaphragm [In Russian]. Moscow: FIAN Preprint; 1985; 254.
6. Clark PP, Howard JW, Freniere ER. Asymptotic approximation to the encircled energy function for arbitrary aperture shapes. *Appl Optics* 1984; 23(2): 353-7.
7. Willis HF. A formula for expanding an integral as a series. *Philosophical Magazine* 1948; 39: 455-9.
8. Harvey JE, Ftaclas C. Diffraction effects of telescope secondary mirror spiders on various image-quality criteria. *Appl Optics* 1995; 34(28): 6337-49.
9. Orlov EP, Sizova IM. The similarity of statistical properties of narrow-band random processes with arbitrary spectra. Part I. Compact spectra [In Russian]. Moscow: FIAN Preprint; 2010; 14.
10. Orlov EP, Sizova IM. The similarity of statistical properties of narrow-band random processes with arbitrary spectra. Part II. Non-compact diachromic spectra [In Russian]. Moscow: FIAN Preprint; 2011: 18.
11. Sizova IM. On the approximation of some integrals in the theory of light diffraction by apertures with complicated shapes [In Russian]. Moscow: FIAN Preprint; 2014: 16.
12. Sizova IM. On the approximation of some integrals in the theory of light diffraction by apertures with complicated shapes. One more model [In Russian]. Moscow: FIAN Preprint; 2015: 2.
13. Sizova IM. Approximation of encircled energy function in the far-field Fraunhofer zone under the diffraction of plane light wave on plane apertures of complicated shapes [In Russian]. Moscow: FIAN Preprint; 2015: 5.
14. MacKinnon RF. The asymptotic expansions of Hankel transforms and related integrals. *Mathematics of Computation* 1972; 26(118): 515-27.
15. Abramovitz L, Stegun IA (eds). Handbook of mathematical functions. National Bureau of Standards: Applied Mathematical Series-55; 1964; Chap. 9.